

# Activation studies on titanium anodes used in MnO<sub>2</sub> electrodeposition

M. E. ARMACANQUI, R. J. EKERN

RAYOVAC Corporation, Madison, WI 53711, USA

Received 20 May 1991; revised 12 September 1991

Titanium anodes from the electrolysis of electrolytic manganese dioxide (EMD) were activated chemically and electrochemically. The surfaces of activated and nonactivated titanium were characterized. Unlike nonactivated titanium, activated titanium evolved hydrogen and displayed a steady open circuit voltage. Hydrides precipitated on both activated and nonactivated surfaces. The passivating film grown on the anode during EMD deposition thinned during partial cathodic reduction and changed in composition from TiO<sub>2</sub> to TiO<sub>x</sub>. Titanium anodes precoated with a thin layer of MnO<sub>2</sub> showed a delay in cathodic activation proportionally to the thickness of the precoat. A considerable difference in hydrogen diffusivity through thin and thick precoats is inferred from the time delay to activate the titanium surface.

## 1. Introduction

Electrolytic manganese dioxide (EMD) is the principal cathodic material in primary batteries; some 200 000 tons are produced each year. Titanium metal is almost exclusively used now as an electrode for the deposition of EMD from acid electrolytes of MnSO<sub>4</sub>. The advantages [1, 2] of titanium over other materials, such as graphite, include an anode with enhanced chemical stability, fewer impurities in the EMD, an EMD with a more consistent crystallographic structure, and, most importantly, an EMD with dramatically enhanced electrochemical activity. Unfortunately, titanium anodes eventually passivate to an extent which affects the quality of the EMD.

The passivation of titanium in the electrolyte leads to increased microporosity and decreased consistency of the EMD crystallographic structure which degrades the EMD electrochemical performance. The time to passivation for a newly installed set of titanium anodes depends on many factors, including the current density, the electrolyte composition, bath temperature, surface condition and composition, and prior history of the anode. An extension of the time to passivation can be achieved by precoating the electrode [3] for example, with a thin layer of EMD.

Periodic rejuvenation of titanium anodes negates the effects of passivation, at least for some limited time following rejuvenation. Reactivation of passivated titanium can be accomplished by chemical etching or by cathodic reduction [4, 5]. Both processes induce activation by partial removal of the passivating film. In this study, both processes were used to induce the activated state of titanium anodes with different initial surface conditions: (a) sandblasted, (b) passivated, and (c) EMD coated.

## 2. Experimental procedure

The titanium anodes were commercially pure, with about 1 cm<sup>2</sup> of the sandblasted surface exposed during the laboratory electrolysis of EMD. Graphite was the cathode in the electrolysis cell. The electrolyte was 1 M MnSO<sub>4</sub> in 0.3 M H<sub>2</sub>SO<sub>4</sub>, made from analytical grade reagents and deionized water. Bath temperature was 90 ± 2°C.

Activation by chemical etching was done in a diluted solution of 35% HNO<sub>3</sub> and 5% HF, at room temperature. Activation by cathodic reduction was done galvanostatically using a potentiostat. Some samples were cathodically reduced after depositing EMD at 2 mA cm<sup>-2</sup> for various times, to produce precoats of various thicknesses. Prior to coating, the titanium surface was cathodically activated at 5 mA cm<sup>-2</sup>. The thicknesses of relatively thick EMD deposits were determined by weight loss measurements after dissolving the EMD in hot, diluted HCl and presuming theoretical density for the deposit. These measurements were complemented with analytical chemistry. The thicknesses of deposits less than about 50 μm were estimated based on the deposition time relative to deposition times of thicker deposits, presuming a linear relationship between time and thickness under constant electrolysis conditions. Electrode voltages were measured relative to a saturated Ag/AgCl reference electrode. Compositional changes of the electrode surface due to passivation [6, 7] and reduction [8, 9] were characterized by X-ray photoelectron spectroscopy (XPS) and X-ray diffraction (acceleration voltage: 40 kV, current: 25 mA, target: copper, unless otherwise indicated).

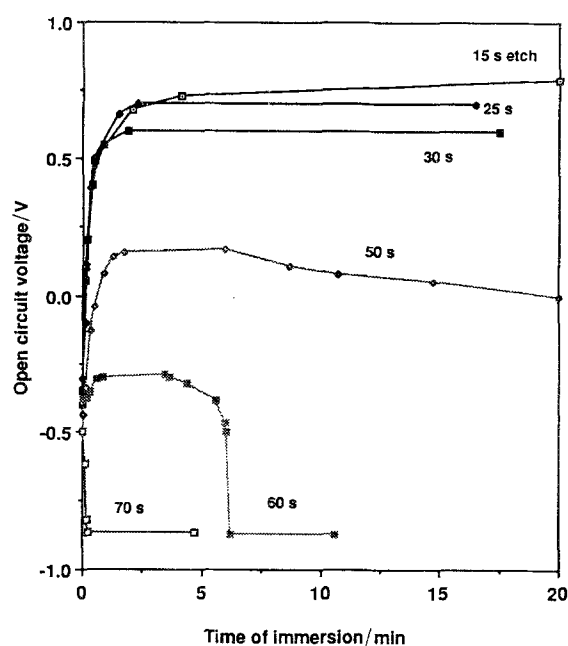


Fig. 1. Open circuit voltage of titanium in electrolyte (0.3 M  $\text{H}_2\text{SO}_4$  + 1 M  $\text{MnSO}_4$  at  $90^\circ\text{C}$ ) after chemical etching for various times in seconds.

### 3. Results and discussion

#### 3.1. Sandblasted titanium

As-received sandblasted titanium displayed an open circuit voltage of approximately  $0.9 \pm 0.05$  V. This value changed only slightly during immersion in the electrolyte. The voltage of etched samples turned in the active direction soon after being immersed in the electrolyte. In the activated state, the voltage was steady at  $-0.8 \pm 0.05$  V and hydrogen gas evolved from the titanium surface. The time necessary to reach the activated state varied from few seconds to many hours depending on the etching time, as seen in Fig. 1. The voltage curves of samples etched for 50 and 60 s suggest that the activation is accelerated after a critical thickness of oxide is reached by the etching.

As in the case of chemical activation, cathodic activation caused a steady negative voltage and hydrogen gas evolution from the titanium surface at open circuit (Fig. 2). The evolution of hydrogen is a consequence of the hydrogen recombination reaction subsequent to the discharge of hydrogen at the solution interface of the oxide film [10]. The evolution became evident only in the latter stages of the activation process, perhaps favoured by the attainment of a new surface composition relative to the initial starting composition [11]. In order to reach the activated state, the applied cathodic current needed to be held for some time beyond that at which the voltage became steady. Figure 3 shows this for a sample cathodically reduced at  $-10 \text{ mA cm}^{-2}$ . At this current density the voltage turned anodic when the cathodic current was interrupted after about 2.1 min of reduction. The calculated time to reach activation [12] at this current density should be about 2.4 min. Figure 4 is a plot of the inverse of the time to reach activation against the

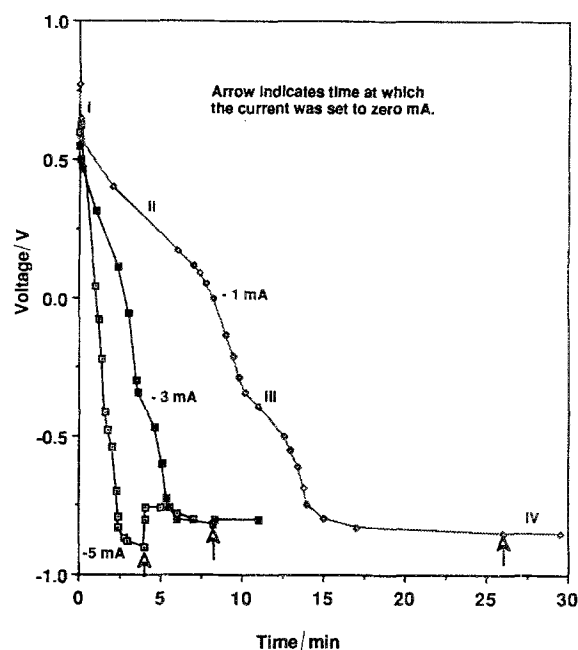


Fig. 2. Voltage of titanium in electrolyte during cathodic reduction at different current densities.

applied current density. The slope and intercept of this curve with the  $y$ -axis was used to estimate the film thickness before cathodic reduction. This thickness was found to be around 8 nm.

Four stages can be identified in the voltage-time curve of titanium during cathodic reduction. This is seen in Fig. 2 for a cathodic applied current density of  $-1 \text{ mA cm}^{-2}$ . The depicted regions resemble those identified by Blackwood *et al.* for the case of open circuit reduction of passivating films on titanium in hot acidic electrolytes [12]. The dominant reaction during the early stages of activation is considered to be a reduction of titanium (IV) oxide to a lower oxidation state followed by chemical dissolution [13, 14]. Region IV, corresponding to the activated state, is the stage of free dissolution of the metal. Nothing definite is known about the surface condition in this stage. Some indicate that in stage IV titanium carries a thin layer of reduced oxide [11, 13] and others believe that no

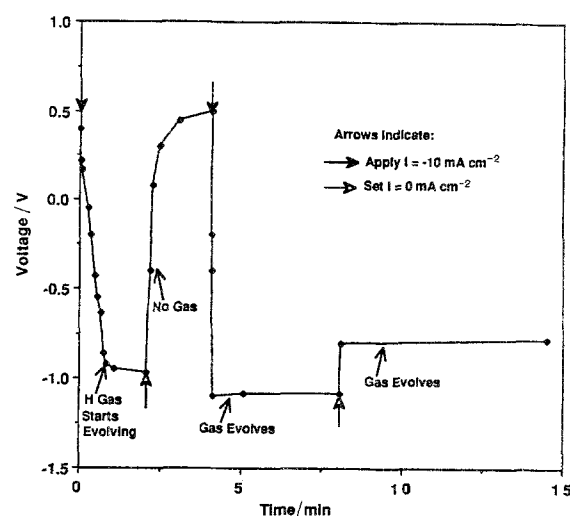


Fig. 3. Voltage of titanium during cathodic reduction at  $-10 \text{ mA cm}^{-2}$ .

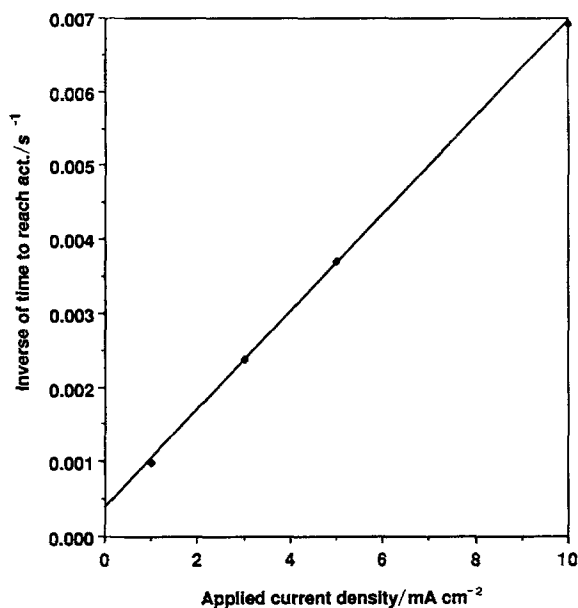


Fig. 4. Inverse of time to reach activation at various applied cathodic current densities.

oxide is present [12, 15]. Just prior to reaching the activated state, the titanium voltage, indicative of the surface condition, did not change in going from the unactivated to the activated state. This is illustrated in Fig. 2 for the sample reduced at  $-1 \text{ mA cm}^{-2}$  and whose activation occurred after 17 min of reduction (Fig. 4). This implies that the surface composition is probably the same right before and during the activated state. In this state some film thinning may take place at a slow rate, as others suggest [5, 16].

During cathodic reduction, the discharge of hydrogen ions at the solution-oxide film interface is followed by their migration through the film to cause hydride precipitation at the metal-oxide interface [17, 18]. An extreme case is that represented by Fig. 5 which shows a diffractogram of titanium after cathodic reduction at  $-5 \text{ mA cm}^{-2}$  for 22 h. Only diffraction peaks of a cubic phase are seen corresponding to a hydride of composition  $\text{TiH}_{1.6}$ . At  $25^\circ \text{C}$ , the air-

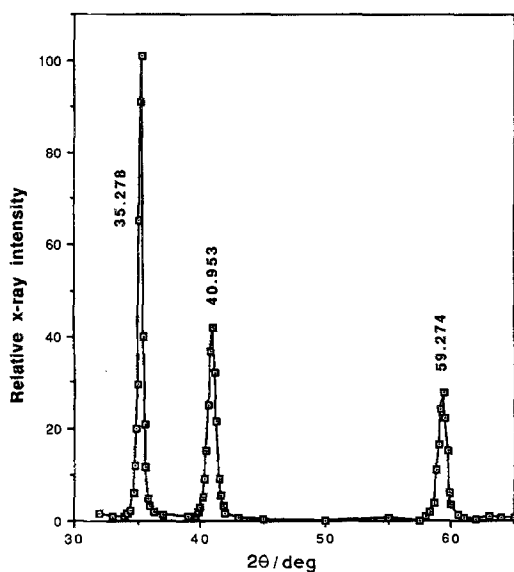


Fig. 5. Diffractogram of titanium after cathodic reduction for 22 h at  $-5 \text{ mA cm}^{-2}$ . Only diffraction peaks of a cubic titanium hydride are seen.

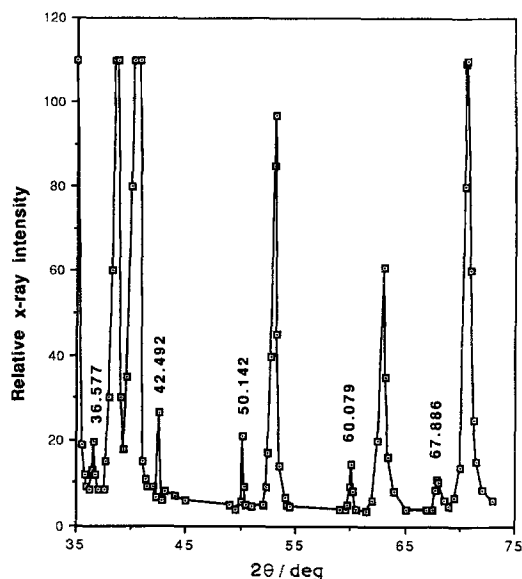


Fig. 6. Diffractogram of nonactivated titanium after open circuit immersion for 25 h in  $0.3 \text{ M H}_2\text{SO}_4 + 1 \text{ M MnSO}_4$  at  $90^\circ \text{C}$ . The weak diffraction peaks belong to hydrided titanium and the strong peaks to the pure metal.

formed surface oxide is believed to inhibit hydrogen absorption by the metal [18, 19]. This does not seem to be the case at  $90^\circ \text{C}$ . At this temperature, open circuit immersion of nonactivated titanium for 25 h caused hydride precipitation. The respective diffraction pattern is given in Fig. 6. The strong diffraction peaks correspond to titanium and the weak peaks showing the diffraction angles belong to the hydride.

### 3.2. Passivated titanium

Galvanostatic deposition of EMD at  $19 \text{ mA cm}^{-2}$  passivated the titanium surface and induced a rapid increase in voltage after about 1.5 h. After scraping the EMD deposit, a bluish or yellowish oxide, or a mixture of both, was found on the titanium surface. The application of cathodic currents to the scraped surface caused rapid reduction of the oxide film. At a cathodic current of  $-5 \text{ mA cm}^{-2}$ , the activated state was reached in less than 15 min. This reduction time differed by less than 10 min from that corresponding to as-received titanium (Fig. 7). Figure 7a shows the voltage curve during cathodic reduction of passivated titanium and figure 7b corresponds to that of titanium reduced in the as-received condition. The passivated sample was deposited with EMD for 8 h and the deposit scraped prior to reduction.

Analysis of the passivated titanium surface by XPS after scraping the EMD deposit gave a pattern equivalent to that of  $\text{TiO}_2$ . This is seen in Fig. 8a for a sample passivated during deposition for 5 h at  $19 \text{ mA cm}^{-2}$ . Partial cathodic reduction at  $-5 \text{ mA cm}^{-2}$  of another as-deposited sample for 21 h left a yellowish oxide after scraping the deposit. This oxide of unknown composition  $\text{TiO}_x$  gave a XPS pattern which was shifted relative to that of  $\text{TiO}_2$  (Fig. 8b). It is not certain whether the film of composition  $\text{TiO}_x$  was a result of the cathodic reduction or formed during EMD deposition as a suboxide layer between the metal and the

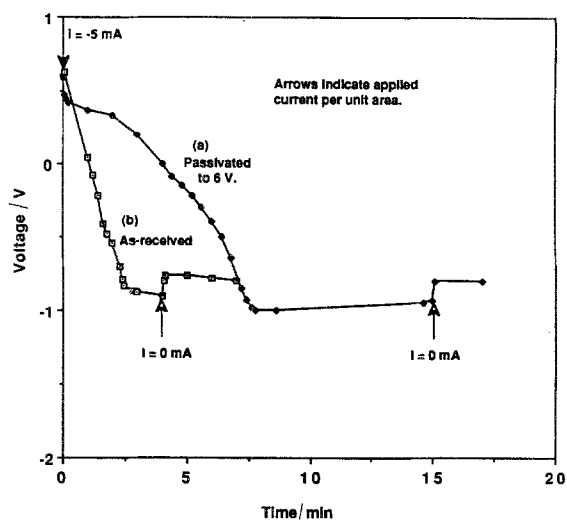


Fig. 7. Voltage during cathodic reduction at  $-5 \text{ mA cm}^{-2}$  of (a) passivated nonprecoated titanium and (b) as-received nonprecoated titanium.

dioxide film [8]. X-ray diffraction done on the passivated 8a sample revealed three weak peaks, in addition to the titanium peaks. These weak peaks, with interplanar lattice spacing of 0.334, 0.245, and 0.167 nm, correspond approximately to the three strongest peaks of rutile. Figure 9 shows two of these peaks at 26.656 and 36.632  $2\theta$  degrees along with few titanium peaks. Evidence of electrochemical formation of rutile on titanium has also been given by others [20]. On the other hand, the x-ray diffraction profile from the partially reduced sample 8b showed only titanium peaks. Based on the deposition time, one expects the oxide film thickness on sample 8b to be greater than that on sample 8a. This suggests that the partial cathodic reduction applied to sample 8b deposited with EMD caused considerable thinning of the oxide.

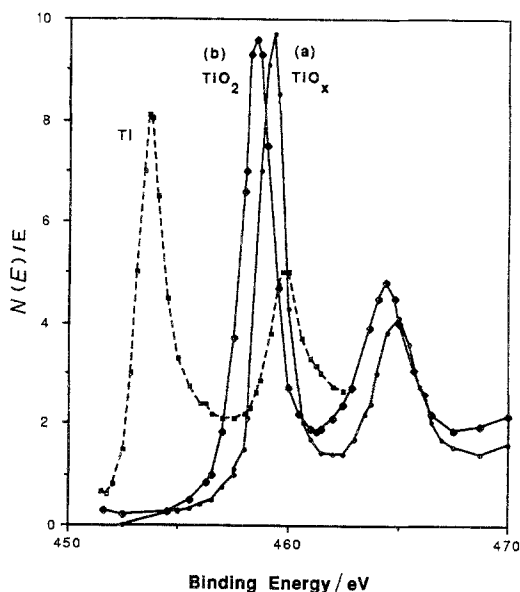


Fig. 8. XPS pattern of (a) passivated titanium and (b) partially reduced passivated titanium. Both samples were passivated during EMD deposition at  $19 \text{ mA cm}^{-2}$  for 5 h and 21 h, respectively.

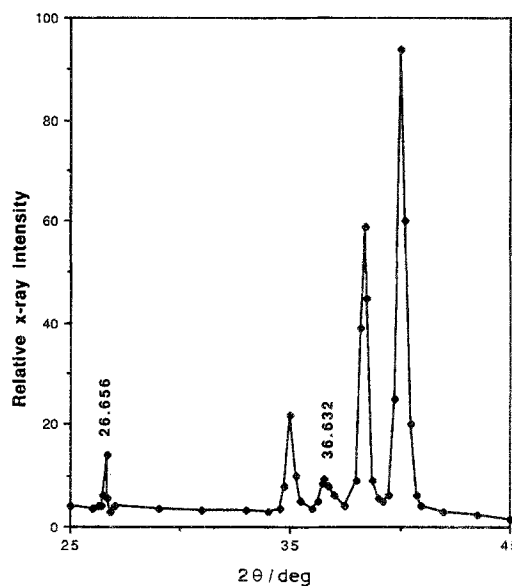


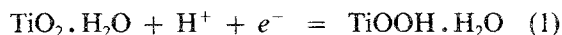
Fig. 9. Diffractogram of sample 8a passivated during EMD deposition at  $19 \text{ mA cm}^{-2}$  for 5 h.

### 3.3. EMD-coated titanium

The applied anodic current of  $2 \text{ mA cm}^{-2}$  to coat titanium with EMD would also induce oxide growth on titanium underneath the coating. However, the oxide growth is expected to be rapidly suppressed by the growing  $\text{MnO}_2$  at this relatively low deposition current density [21].

Cathodic reduction of EMD-coated titanium caused the voltage to drop after some time of reduction and hydrogen to evolve immediately after. The coating detached from the substrate at the time hydrogen started to evolve. The pressure exerted by the evolving hydrogen probably caused the EMD to break away from the substrate.

The applied cathodic current to EMD-coated titanium would cause some reduction of the EMD layer of  $\text{MnO}(\text{OH})$  [22]. Some hydrogen ions also would diffuse through the coating to the oxide-EMD interface to cause reduction of the underlying oxide according to [11]



Assuming that a negligible thickness of oxide grows during coating and that reduction of this film occurs almost instantly, reduction of EMD-coated titanium is expected to be completed at the time immediately following the voltage drop to the negative steady value. Accordingly, the voltage was found to remain steady after the applied current was interrupted at the referred time. This time was taken as the approximate time to reach the activated state of EMD-coated titanium. This time would also be the approximate diffusion time of hydrogen to the oxide-EMD interface, assuming that the coating thickness was unaffected by the reduction, as confirmed by an individual measurement. If the hydrogen diffusivity is independent of EMD thickness, a plot of the EMD coating thickness as a function of the square root of time to reach the activated state should give a linear

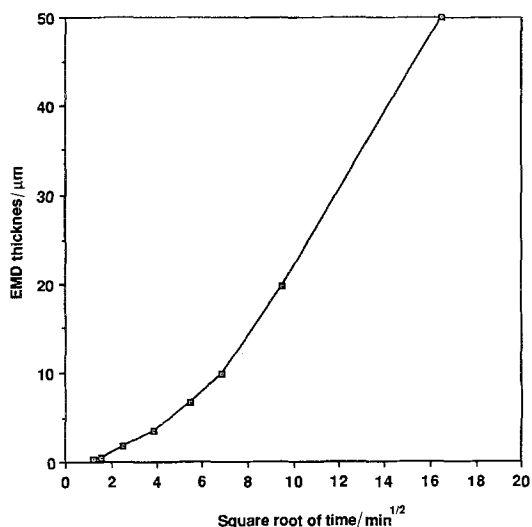


Fig. 10. EMD coating thickness against the square root of time necessary to reach activation during cathodic reduction at  $-5 \text{ mA cm}^{-2}$ .

relationship. However, this was found not to be the case, as can be seen in Fig. 10. The reported diffusion coefficient for protons in  $\text{MnO}_2$  of about  $6 \times 10^{-10} \text{ cm}^2 \text{ s}^{-1}$  [23] is probably an average value. The hydrogen diffusivities of EMD coats thinner than  $5 \mu\text{m}$  appear to be at least one order of magnitude less than the reported value.

Among other things, the apparent thickness dependence of the hydrogen diffusivity may be a result of the finding that the crystal structure of EMD was not uniform. The x-ray diffraction pattern of thick EMD layers taken from the surface that was directly in contact with the electrolyte showed diffraction peaks of predominantly orthorhombic  $\gamma\text{-MnO}_2$  (Fig. 11a), considered to be the most favourable structure for insertion [24, 25] from the point of view of site availability and rate of diffusion. The diffraction pattern taken from the EMD surface that was in contact with the

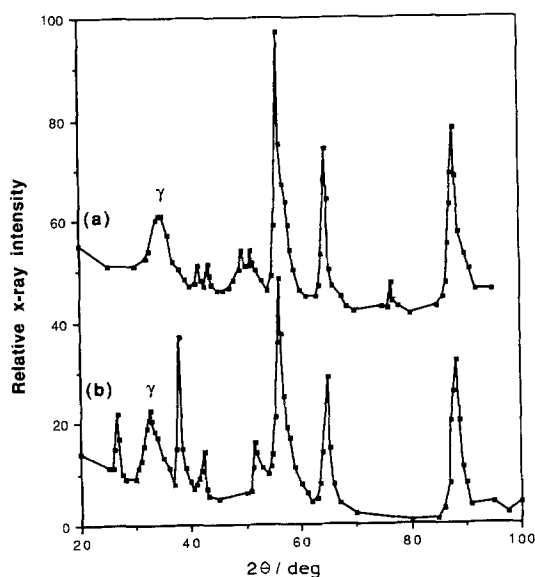


Fig. 11. Diffractogram of EMD taken from (a) the surface in contact with the electrolyte, and (b) the surface directly in contact with the substrate.

titanium substrate was different than that of  $\gamma\text{-MnO}_2$ , as seen in Fig. 11b. The diffraction profile in Fig. 11b can not be ascribed to a unique known phase. New peaks appear in the neighbourhood of the characteristic  $\gamma\text{-MnO}_2$  peak at  $33.30 \text{ } 2\theta$  degrees (chromium target). Although the position of these new peaks are close to those belonging to cryptomelane  $\alpha\text{-MnO}_2$  of tetragonal structure, the relative intensity of the peak at about  $38 \text{ } 2\theta$  degrees is unusually high with respect to the others nearby. At this angle of diffraction, two peaks may be overlapping, one of which could belong to  $\delta\text{-MnO}_2$  [26]. One can also notice in Fig. 11b a small shift in the depicted  $\gamma$  peak position and some changes relative to the line shape of the diffraction peaks shown in Fig. 11a.

During the growth of the EMD layer, one can envision changes in the EMD lattice structure during the early stages of deposition to become predominantly  $\gamma\text{-MnO}_2$  at a later stage. The apparent changes in lattice structure during growth may be related to the defect concentration in the EMD. It has recently been shown that the structure of  $\text{MnO}_2$  is very much dependent on the defect density present in the EMD [27]. Calculations of the diffraction profiles of  $\text{MnO}_2$  as a function of defect concentration have shown that the diffraction lines of the  $\gamma$  phase experience a shift and a change in width as the amount of faults increases in the material. This would suggest a high lattice defect concentration in EMD near the substrate and not as much away from the substrate. Because of trapping effects, the diffusivity of hydrogen in the highly defective structure can be few orders of magnitude smaller than that in the less defective structure [28, 29].

#### 4. Conclusions

The activated state of titanium after chemical or electrochemical reduction is characterized by a steady voltage and hydrogen evolution at open circuit. During immersion at open circuit, precipitation of hydrides occurs on activated titanium and, to a lesser extent, on nonactivated titanium. The electrolytic deposition of  $\text{MnO}_2$  on titanium causes passivation of the surface with a film of rutile  $\text{TiO}_2$ . Partial cathodic reduction of passivated titanium results in thinning of the passivating film and the appearance of an oxide different than  $\text{TiO}_2$ . An apparent thickness dependence of hydrogen diffusivity in  $\text{MnO}_2$  is inferred from the cathodic reduction of  $\text{MnO}_2$  coated titanium. This may be related to the nonuniform structure of  $\text{MnO}_2$  which results from coating to titanium.

#### Acknowledgements

The authors acknowledge the support of the RAYOVAC Corporation for this work. The assistance of T. J. Stachowiak in chemical analysis is also acknowledged.

#### References

- [1] E. Preisler, *J. Appl. Electrochem.* **19** (1989) 540.

- [2] *Idem*, *J. Appl. Electrochem.* **19** (1989) 559.
- [3] F. A. Kalinoskii, Y. K. Rossinskii and Z. M. Kebabze, *Z. Prikladnoi Khim.* **61** (1988) 293.
- [4] C. P. De Pauli, M. C. Giordano and J. O. Zerbino, *Electrochim. Acta* **28** (1983) 1781.
- [5] T. Ohtsuka, M. Masuda and N. Sato, *J. Electrochem. Soc.* **134** (1987) 2406.
- [6] D. J. Blackwood, R. Greef and L. M. Peter, *Electrochim. Acta* **34** (1989) 875.
- [7] J. L. Delpancke and R. Winnand, *ibid.* **33** (1988) 1539.
- [8] D. J. Blackwood, L. M. Peter, H. E. Bishop, P. R. Chalker and D. E. Williams, *ibid.* **34** (1989) 1401.
- [9] W. Wihelmsen and A. P. Grande, *ibid.* **35** (1990) 1913.
- [10] R. M. Torresi, O. R. Camara and C. P. De Pauli, *ibid.* **32** (1987) 1291.
- [11] J. A. Harrison and D. E. Williams, *ibid.* **27** (1982) 891.
- [12] D. J. Blackwood, L. M. Peter and D. E. Williams, *ibid.* **33** (1983) 1143.
- [13] C. K. Dyer and J. S. L. Leach, *ibid.* **23** (1978) 1387.
- [14] *Idem*, *J. Electrochem. Soc.* **125** (1990) 23.
- [15] L. D. Arsov, *Electrochim. Acta* **30** (1985) 1645.
- [16] D. Laser, M. Yaniv and S. Gottesfeld, *J. Electrochem. Soc.* **125** (1978) 358.
- [17] R. M. Torresi, O. R. Camara, C. P. De Pauli, *Electrochim. Acta* **32** (1987) 1291.
- [18] T. Okada, *ibid.* **27** (1982) 1273.
- [19] P. G. Pound, *Corrosion* **47** (1991) 99.
- [20] A. Felske and W. J. Plieth, *Electrochim. Acta* **34** (1989) 75.
- [21] J. Petitpierre, C. Comminellis and E. Plattner, *Electrochim. Acta* **35** (1990) 281.
- [22] F. A. Kalinoskii, Yu. K., Rossinskii, V. A. Shustov and Zh. M. Kebabze, *Z. Prikladnoi Khim.* **61** (1988) 299.
- [23] H. Kahil, F. Dalard, J. Guittou and J. P. Cohen-Addad, *Surf. Technol.* **16** (1982) 331.
- [24] M. Voinov, *Electrochim. Acta* **26** (1981) 1373.
- [25] *Idem*, *ibid.* **27** (1982) 833.
- [26] Proceedings of the Symposium on the Manganese Dioxide Electrode Theory and Practice for Electrochemical Applications, Electrochemical Society, **85-4** (1985) 280.
- [27] J. Pannetier, 'Solid State Ionics No 2', Materials Research Society Symposium Proceedings, **210** (1991) 359.
- [28] W. D. Wilson, S. C. Keeton, in 'Advanced Techniques for Characterizing Hydrogen in Metals', (edited by N. F. Fiore, B. J. Berkowitz), Symposium Proceedings, AIME, Kentucky, (1981) p. 3.
- [29] B. G. Pound, *Corrosion* **45** (1989) 18.